A Bio-Inspired Slip Detection and Reflex-Like Suppression Method for Robotic Manipulators

Andrei Nakagawa-Silva, Nitish V. Thakor, *Life Fellow, IEEE*, John-John Cabibihan, *Senior Member, IEEE*, and Alcimar B. Soares, *Member, IEEE*

***Abstract*— Robotic manipulators face significant challenges when handling objects of different sizes and shapes. Incorporating a sense of touch into these devices has the potential to improve performance and dexterity. In this paper, a bio-inspired approach is presented for slip detection and suppression during object manipulation. The method was inspired by the behavior of FA-I afferents located in the glabrous skin that encode sliding motion of objects over the skin. The proposed slip detection method encodes object motion captured by a slip sensor into spikes, following principles of neuromorphic sensing. The spikes are used as the feedback signal for an event-based closed-loop control system. The controller behaves in a reflex-like manner and actively engages the robotic fingers to increase grip force and suppress slip. A Dynamic Adaptive Threshold method was designed to improve slip detection for different surface properties of grasped objects. The performance of the method was evaluated following situations of dynamic slip caused by a sudden or gradual increase in object weight. The results demonstrated the feasibility of the proposed method. Slip events were suppressed before complete object slippage in 80% of all experimental trials. The response time (Δt < 85 ms) was compatible with the time for grip force adjustments in humans. This paper explored event-based touch applicable to the problem of manipulation, which is less explored than event-based tactile perception and shows promising prospects for both robotics and prosthetics.**

***Index Terms*— Event-based, prosthetics, robotics, slip detection, tactile sensing.**

I. Introduction

THE human hand is remarkable for its manipulation skills. The sense of touch is largely involved in sophisticated dexterity, using thousands of mechanoreceptors located on the skin to encode contact-based information that is crucial for proper manipulation of objects and tools. These specialized receptors encode the roughness, friction, hardness, and spatial structure (edges, gratings) of surfaces [1]. Such information is essential for grasp planning and control of the grip force during manipulation tasks [2]. Westling and Johansson [3] demonstrated that, in humans, the grip force is adjusted depending on the friction properties of the surface, where more slippery textures invoke higher grip forces. Moreover, the above-mentioned authors showed that the grip force is slightly higher than the minimum required to prevent slippage of objects. Likewise, grip force adjustments occur between 60-80 ms after slip onset [4], [5]. Despite the importance of the sense of touch, robotic manipulators and prosthetic hands have not yet been fully equipped with tactile capabilities, especially those using high-density or rapidly adapting sensors that could improve their manipulation skills.

Research on artificial tactile sensing has increased over the past few decades [6]. A variety of tactile sensors can be found in the literature with applications that involve preventing excessive grip force [7], texture recognition [8], and delivering tactile feedback to amputees [9]. The use of tactile sensors affords a good prospect for improving grasp stability during manipulation, especially when dealing with objects of different sizes and shapes. One of the key elements for grasp stability is the detection of slip caused by inappropriate grip force or unexpected disturbances [10].

Slip is characterized as a fast, transient event caused by the break of contact between the end-effector and the object being grasped. In such cases, it is required to adjust grip force to recover stability properly. Different types of sensors and methods have been proposed to create an artificial sense of slip [11]–[13]. When using force sensors, a sudden drop in the force signal usually indicates slip, which is detected after it crosses a threshold or an increase in power of high-frequency components caused by vibrations occurs [14]–[16]. In contrast, optical sensors provide the capacity of accurately tracking object motion [17], [18]. These sensors have the advantage of offering a continuous output over the entire course of slip instead of a more discrete-like response generated by taking the derivative of the sensed force. Continuous output can be better exploited by control systems that act as to prevent the complete slippage of objects. However, optical sensors are limited by their sensitivity to the reflectance properties of the objects [17].

In humans, sliding motion and slip are captured by Meissner Corpuscles and Merkel Cells. Meissner Corpuscles are fast adapting (FA-I) receptors, tuned to transient stimuli,

Manuscript received August 8, 2019; accepted August 19, 2019. Date of publication September 4, 2019; date of current version November 26, 2019. This work was supported in part by the Office of Naval Research (ONR Global-USA) under Grant N62909-15-1-2024 and in part by the Qatar National Research Fund (QNRF) under Grant 7-673-2-251. The work of A. Nakagawa-Silva and A. B. Soares was supported in part by Coordenação de Aperfeiçoamento de Pessoal de Nível Superior (CAPES), Brazil, through DS Program Port #76 and in part by Conselho Nacional de Desenvolvimento Científico e Tecnológico (CNPq), Brazil, under Grant 428291/2016-3 and Grant 311273/2018-1. The associate editor coordinating the review of this article and approving it for publication was Dr. Sanket Goel. *(Corresponding author: Andrei Nakagawa-Silva.)*

A. Nakagawa-Silva and A. B. Soares are with the Biomedical Engineering Laboratory, Faculty of Electrical Engineering, Universidade Federal de Uberlândia, Uberlândia 38400-902, Brazil (e-mail: andrei.ufu@gmail.com).

N. V. Thakor is with the Biomedical Engineering Department, Johns Hopkins University, Baltimore, MD 21218 USA, and also with the Singapore Institute for Neurotechnology, National University of Singapore, Singapore 119077.

J.-J. Cabibihan is with the Department of Mechanical and Industrial Engineering, Qatar University, Doha, Qatar.

Digital Object Identifier 10.1109/JSEN.2019.2939506

and provide information regarding motion across the skin, vibration, and delicate texture. Merkel cells are slow adapting receptors (SA-I afferents) and relay information associated with more static stimuli, such as stretching of the skin. The behavior of such mechanoreceptors has inspired novel biomimetic strategies for artificial tactile sensing [19].

Romano *et al.* [20] incorporated a control scheme that separated grasping into six discrete states (close, load, lift and hold, replace, unload, and open) [21]. They used signals captured by pressure arrays mounted on the gripper's fingertip to generate tactile information mimicking the activity of SA-I and FA-I afferents and to move between the states. Their paper demonstrated the feasibility of a tactile-event-driven model for grasp control, suggesting its usefulness for robotic manipulators. Su *et al.* [22] used a biomimetic tactile sensor for force estimation and slip detection. The slip detection method consisted of identifying changes in the amplitude of the force signal caused by high-frequency oscillations that exceeded a threshold. One drawback of this approach is that it can be affected by vibrations applied to objects that are caused by the motors or external disturbances without actual slip. Osborn *et al.* [7] used a neuromimetic strategy for improving grasp control of a prosthetic hand, drawing inspiration from the information encoded by SA-I and FA-I afferents. The authors used the force signal measured by a piezoresistive tactile sensor to prevent excessive grip force and detect slip. The derivative of the force signal was used to highlight transient aspects of the signal. A slip was detected by monitoring changes in the derivative that exceeded a certain threshold. After slip was detected, the prosthesis received a command to close the fingers and prevent complete slippage of the object. Given the discrete nature of their strategy, the method was not sensitive to the magnitude of the slip, generating the same response regardless of how much the objects would slip.

This paper further advances the bio-inspired approach for tactile sensing and presents a slip detection method that is combined with a closed-loop control system to suppress slippage of objects for robotic hands. The proposed system behaves as a low-level reflex-like response that increases grip force in response to slip. Three main contributions are presented: A) An event-based approach for slip detection that produces a response akin to the behavior of FA-I afferents during sliding motion of objects, providing events during object slippage; B) an optical method that improves slip detection to less reflective surfaces; and C) an experimental validation of the Monotonic Proportional-Integral (MPI) control law [23] for effective slip suppression. The slip detection method generates discrete events based on the analog output signal of a slip sensor as the motion between the object and the end-effector is perceived [24]. Motion is captured by the sensor due to surface anisotropies and texture of the object, which change the direction and the amount of the reflected light from the object's surface. Such changes are observed as fluctuations in the amplitude of the slip sensor signal. This approach renders the method invariant to the absolute amplitudes of the sensor, automatically segments the signal by indicating the absence or presence of slip and rejects fluctuations caused by electrical or mechanical noise. In this sense, the proposed method implements a novel neuromorphic approach to tactile sensing.

The majority of the works published in the field of neuromorphic tactile sensing have been focused mainly on converting the output of force sensors into spikes for applications such as texture recognition ([8], [25]), and Gait event detection [26]. In this paper, the focus is on encoding sliding motion associated with slip. In a previously published work, a significant decrease in sensitivity was observed when this strategy was applied for transparent objects [27]. In order to overcome such limitations, a Dynamic Adaptive Threshold (DATH) method is proposed to improve slip detection and suppression for less reflective surfaces. Whenever an event is captured, the threshold for generating events changes over a short time window to amplify its sensitivity temporarily. The slip detection method was combined with the MPI control law for preventing complete object slippage. The MPI controller was modified to an event-based control system by using the number of slip events as input. Experimental evidence of the model's feasibility is provided by analyzing its performance during situations of dynamic slip caused by a sudden or gradual increase in object weight, demonstrating its effectiveness for such purpose.

II. Materials and Methods

A. Hardware Design and Data Acquisition

In this study, three primary elements were used: the slip sensor, which consisted of an optical sensor (OPR 5005 - TT Electronics, UK) alongside its driver circuit, a data acquisition system and a real-time control loop operated via software. The OPR 5005 is a miniature diffuse reflective optical sensor that combines an Infrared LED and a phototransistor in the same package. The sensor was chosen given its simplicity and small package size that makes it easy to be mounted in any robotic manipulator. The characteristic output of the sensor was found by taking its average response when tested on surfaces of different reflectance properties (current limiting resistors were used for both the IR LED (100 Ω) and the phototransistor (4.7 kΩ)). The analog voltage was read from a data acquisition board (10-bit Analog to Digital Converter - ADC) equipped with an 8-bit Atmel AVR microcontroller, which was also used to obtain data from a water flow sensor (YF-S201) and an inertial measurement unit (IMU) (MPU6050, InvenSense, USA). The samples were digitalized at 333 Hz and sent to the PC via USB. A custom software was developed in Python 3.6.5 to record data and also run the slip detection and suppression methods in real-time. Fig. 1 presents an overall view of the hardware setup used in this work.

B. Robotic Hand

In this work, a prosthesis control unit (Infinite Biomedical Technologies, Baltimore, USA) is used to interface with an i-Limb prosthetic hand (Touch Bionics, UK). The i-Limb can be operated using commands sent via a serial interface. A framework was developed to control each finger individually with a position-based control. The slip sensor was placed inside a customized 3D printed cuff designed especially for

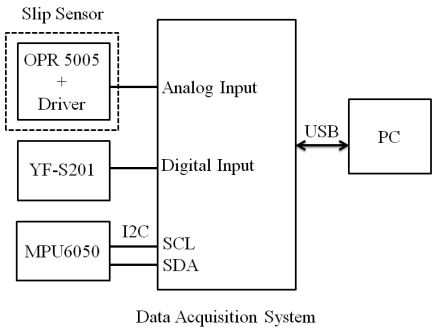

Fig. 1. Block diagram of the hardware setup. The slip sensor is composed of an optical sensor (OPR 5005) and its driver. The data acquisition system reads data from the slip sensor and two other sensors used during the experiments. A digital input is used to read from the YF-S201 water-flow sensor. The I2C protocol is used to communicate with the IMU MPU6050. Data is transferred to the PC in real-time via USB. The software implements both the event-based slip detection procedure and the MPI control law.

Fig. 2. Sensor placement on the i-Limb fingers using customized 3D printed cuffs. A) Tactile sensors are placed on the index finger and the thumb for monitoring the initial contact. The slip sensor is placed on the middle finger (marked in red). B) Detailed view of the slip sensor placed inside a 3D printed cuff.

the dimensions of each finger of the prosthesis. Two additional tactile sensors were placed on the index finger and the thumb. Those sensors have been used only to monitor the force during initial contact between the i-Limb fingers and the objects. The fingers were closed until the tactile sensors detected a contact force of 0.8 N. Fig. 2 shows the tactile sensors mounted on the thumb and index fingers, while the slip sensor was mounted on the middle finger.

C. Slip Detection and Slip Suppression Framework

The proposed method makes use of spikes generated according to the output signal of the slip sensor. The raw output of the slip sensor is first filtered and passed to the bio-inspired event-based slip detection module, which accumulates the difference between consecutive samples. When the accumulated value crosses a threshold, a spike is generated. The number of spikes is used as a feedback signal to the MPI controller, which adjusts the grip force of the i-Limb hand, as shown in Fig. 3.

1) Bio-Inspired Event-Based Slip Detection: The raw analog voltage of the slip sensor can be informative of the motion of an object with respect to the field of view of the sensor. Depending on the surface properties of the object, the voltage level of the response will vary. The sensor is also sensitive enough to produce responses that can be characterized with respect to motion or slip. As described earlier, the proposed slip detection method was inspired by event-based systems. With such an approach, it is possible to highlight the changes

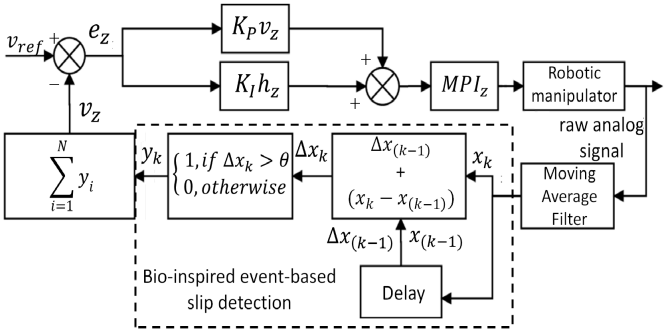

Fig. 3. The proposed framework combines a bio-inspired slip detection method with the MPI control law to prevent object slippage. The raw analog signal is first filtered, and every sample x_k is used to generate spikes. The number of spikes v_z in a given time window is the feedback signal to the controller. The error signal e_z is given by the absolute difference between v_{ref} and v_z. The MPI control law controls the finger positions of the i-Limb and responds to slip by increasing the closure of the fingers and, thus, the grip force.

in sensor readings by converting them into events, or spikes, while avoiding fluctuations caused by noise.

The output signal from the slip sensor is first low-pass filtered (10Hz) during a pre-processing stage. The first step in the slip detection procedure consists of accumulating the instantaneous difference between consecutive samples over time, as shown in Eq. 1. The initial state for the integration is $\Delta x_0 = 0$ and $x_0 = 0$.

$$\Delta x_k = \Delta x_{(k-1)} + \left(x_k - x_{(k-1)}\right), \quad \mathrm{k} \geq 1 \tag{1}$$

where x_k is the current filtered sample of the slip sensor signal, $x_{(k-1)}$ is the previous filtered sample, and Δx_k is the current accumulation value.

The absolute value of Δx_k is compared to a threshold θ. When Δx_k crosses θ, an event or spike ($y_k = 1$) is generated, as shown in Eq. 2. After an event is generated, the value of Δx_k is reset to start a new integration process. The slip detection procedure is described in Eq. 2.

$$y_k = \begin{cases} 1, & if\ |\Delta x_k| > \theta \\ 0, & otherwise \end{cases} \tag{2}$$

where y_k is the output of the event detection method, and θ stands for the threshold that determines the condition for an event to be triggered.

In this work, the detection threshold was set to $\theta = 0.008$. The value of θ was chosen based on the output of the sensor and on the resolution of the ADC (one LSB bit = 0.004 V). After the difference between consecutive sensor readings was measured and compared with the noise level of the circuit, a threshold of twice the voltage level for one LSB was established. This value of θ provides good sensitivity to capture slip events while avoiding false positives.

The output of the event detection method (y_k) is then filtered by counting the number of events that are triggered within non-overlapping windows of 50 ms (N = 16 samples) (Eq. 3). In so doing, the events are smoothed, and become more informative of the motion of the object over time, since the number of spikes can be better related to object motion. Finally, the smoothed events are sent as a velocity signal (v_z) to serve

as input to the MPI controller.

$$v_z = \sum_{i=1}^{N} y_{i,N} \quad (\mathrm{N} \leq 16) \tag{3}$$

2) Dynamic Adaptive Threshold (DATH) for Improved Detection: Optical tracking sensors are, in general, sensitive to the reflectance properties of the surfaces that are placed within their field of view. For instance, transparent and dark objects produce low levels of reflectance, while white objects produce the highest reflectance. From the characterization experiments, it was observed that different surfaces modulated the amplitude of the sensor output due to object motion. Less reflective surfaces produced responses of smaller amplitude than textured or rough surfaces. Nevertheless, although the amplitudes were different, the sensor still produced a good response. However, due to those differences, the fixed threshold (θ) used in the initial model for detecting slip events was not always appropriate, highlighting the need for a dynamic method. To do so, the DATH strategy is activated when a first slip event is detected. After such an event, a new threshold is set based on the instantaneous difference between the current and the previous filtered output sample from the slip sensor (Eq. 4).

$$\theta_{DATH} = \left| x_k - x_{(k-1)} \right| \tag{4}$$

where x_k and $x_{(k-1)}$ refer to the current and previous filtered samples, respectively. DATH amplifies the number of detected events by zooming-in closer to the fluctuation levels of the sensor output, which are related to motion induced by slip. The magnitude of the changes in amplitude due to the surface properties is implicit in Eq. 4. With this method, less reflective surfaces should show a smaller threshold than more reflective surfaces. Furthermore, the increase in sensitivity is temporary and lasts only for 50 ms, which is an appropriate time for the controller to suppress the detected slip events properly. After this period, the threshold is reset back to $\theta = 0.008$ until a new slip event is detected.

3) MPI Controller: The MPI control law proposed by [20] was modified to suit the application in this study, as well as the proposed slip detection method. Accordingly, the MPI control law determines the position of the fingers of the i-Limb. As slip occurs, the value of the MPI output will increase, indicating that the fingers should close more, increasing contact and, consequently, grip force. Thus, the objective of the control system is to regulate the grip force applied by the fingers to bring the number of slip events to zero. The controller generates an output every 50 ms when a new number of slip events (v_z) is generated.

The PI control law is given by Eq. 5:

$$PI_z = K_P e_z + K_I \sum e_z \tag{5}$$

where K_P is the proportional gain, K_I is the integral gain, and e_z is the error signal given by $e_z = v_{ref} - v_z$. Since $v_{ref} = 0$, as the objective is to reduce slip events to zero, then $e_z = -v_z$. Nevertheless, since slip suppression requires an increase in grip force, the absolute value of v_z ($e_z = v_z$) must be used. Therefore, the PI control law can be expressed by:

$$PI_z = P_0 + K_P v_z + K_I h_z \tag{6}$$

where P_0 is the initial position of the fingers and h_z, given by Eq. 7, represents the cumulative sum of the number of slip events captured over time.

$$h_z = \sum_{i=1}^{z} v_i \tag{7}$$

Applying the closed-loop PI control, the transition between mostly proportional to mostly integral action might cause the output of the controller to decrease. In such cases, the grip force would decrease, which might lead to other slip events. Thus, the MPI determines that the output of the controller should increase monotonically with every detected slip event in order to prevent the grip force from decreasing, maintaining grasp stability. The MPI control law is given by Eq. 8, which shows that the actual output of the controller is equal to the maximum value between the current PI output and the previous MPI output.

$$MPI_z = argmax\,(PI_z, MPI_{z-1}) \tag{8}$$

In this work, the control constants were set as $K_P = K_I = 5$. The MPI control law is reset if the velocity remains equal to zero over ten consecutive windows. In such cases, P_0 is set to the current position of the middle finger, and h_z is set to 0. Finally, the output MPI_z is passed to a piecewise linear saturation function (Eq. 9) that guarantees that the control output is within the range of the finger positions (0: finger fully opened; 500: finger fully closed).

$$MPI_z = sat\,(MPI_z) \tag{9}$$

D. Experimental Setup

Two different experiments were conducted to evaluate the effectiveness of the proposed method. First, the response of the slip sensor to motion was characterized, and the performance of the slip detection method was evaluated. The experimental setup consisted of a robotic arm – UR10 (Universal Robots, Denmark) with the slip sensor attached to its end-effector and a 3D printed vertical stand that had a test surface fixated to it. The test surface consisted of white (1 cm long, maximum reflectance) and black (3 cm long, minimum reflectance) portions (Fig. 4A). The vertical stand was placed 3 mm apart from the sensor, which is the same distance given by the gap in the finger cuff, as shown in Fig. 1. The UR10 started at the top portion of the test area and moved 5 cm down along the z-axis in a straight line, at a constant speed of 1 mm/s (Fig. 4B). This scanning procedure promoted relative motion between the sensor and the test surface, changing the patterns of the reflected light detected by the slip sensor. These changes were reflected in the response of the sensor and used to characterize it, in terms of sensitivity and spatial resolution, and to verify whether events related to motion or slip could be generated.

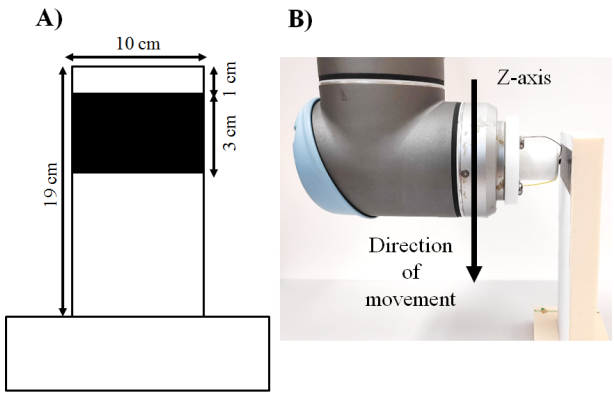

Fig. 4. The experimental setup used to characterize the slip sensor output and evaluate the performance of the slip detection method. A) A 3D printed vertical stand was used to fixate a test surface composed of white and black portions with maximum and minimum reflectance properties, respectively. B) The slip sensor was attached to the end-effector of a UR10 robotic arm at a distance of 3 mm from the stand. During the experiment, the UR10 moved 5cm down along the z-axis at a constant speed of 1 mm/s. The relative motion between the robotic arm and the vertical stand induced changes in the sensor response that were characterized and converted into events by the event-based slip detection method.

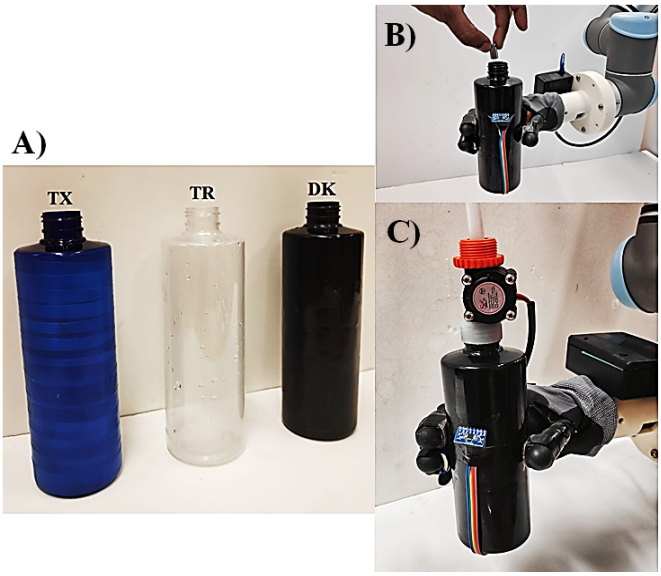

Fig. 5. The experimental setup used for measuring the performance of the slip suppression method. The i-Limb prosthetic hand was mounted on the UR-10. The bottle was grasped with minimal contact using a tripod grasp (thumb, index, and middle finger of the i-Limb). The slip sensor was placed in the middle finger, and the IMU was attached to the bottle in order to determine the onset of slip. A) Three bottles (TX, TR, and DK) were used in the experiments. B) In the first experiment, a standardized object with a mass of 10 g was suddenly dropped into the bottle, triggering a fast slip event. C) In the second experiment, the weight of the bottle was gradually increased by pouring 500 ml of water using a water pump with a constant flow rate (1 L/min). Increasing the weight promoted distinct slips of the bottle over time.

Two proof of concept experiments were performed to demonstrate how the slip detection method could be combined with the MPI controller to suppress complete slippage of objects. Three standard plastic bottles (16 cm height $\times$ 2 cm diameter, 40 g weight) were used for this experiment (Fig. 5A). The bottles were chosen to provide a different range of reflectance properties while maintaining the same overall structure. The first bottle was smooth and transparent (TR), the second one had a smooth and dark surface (DK), and the last one had a textured-rough surface obtained by covering the bottle with blue tapes (TX). In both tasks, object weight was dynamically changed, either suddenly or gradually, triggering unexpected slips.

For the experimental setup, the i-Limb prosthetic hand was attached to the UR10 and used to perform the manipulation tasks. The i-Limb grasped the bottles with minimal contact using a tripod grasp with the slip sensor placed on the middle finger. The first experiment consisted of dropping an object with a mass of 10 g inside the bottle from a height of 2 cm above its opening, which promoted a fast, sudden slip (Fig. 5B). The second experiment consisted of pouring 500 ml of water into the bottles at a constant rate of 1 L/min (Fig. 5C). A slip would occur depending on the weight of the bottle, and the grip force applied. The first experiment served to evaluate the behavior of the controller to sudden perturbations while the latter served to evaluate the controller response over a gradual perturbation. In each experiment, a total of ten trials were repeated for each bottle. The IMU was attached to each bottle and used to measure the response time of the controller, i.e., the elapsed time between the onset of motion caused by slip and the initial changes in finger position due to the controller output. The number of times that slip events were suppressed correctly, and the total time necessary for the controller to entirely suppress slip were also measured. Then, the average response time and the average total time for slip suppression were calculated.

The response time was measured by finding the onset of slip from the accelerometer signal. First, for each trial, the axis of the accelerometer that produced a more significant response during slip was selected. The accelerometer signal was then rectified and low-pass filtered at 30 Hz. Next, a two-step threshold-based detection was employed to determine the onset of slip. In the first step, the value of the threshold was determined based on the average and standard deviation of the first 200 ms of each trial. During this initial phase, the bottle was steady, and there was no slip. The samples that exceeded the threshold were considered as possible onsets of slip. In the second step, the onsets that occurred outside the time interval where slip was induced were removed. Finally, only the first onset candidate that obeyed both rules was considered as the actual onset of slip.

The response time was measured as the time difference between the increment in finger position, given by the MPI controller, and the slip onset. The total controller time was taken as the time difference between the first and last values of the finger positions provided by the MPI controller. In the experiments pouring 500 ml of water, two distinct slips were observed in most of the trials. All slips were analyzed individually, as if they belonged to a separate trial, and were used to find the average response time and average total controller time for the experiments.

E. Comparative Performance Evaluation

To further evaluate the performance of the proposed method for slip detection and suppression, a comparison with two

other methods proposed in the literature was conducted: i) Osborn *et al.* [7] - a biomimetic method for detecting and preventing slippage of objects manipulated by prosthetic hands; ii) Romeo *et al.* [16] – a method based on stationary wavelet transform for fast slip detection. For compatibility throughout the experiments and to provide a fair comparison of performance, the 4×4 (16 taxels) tactile sensor shown in Fig. 2 was used for monitoring force and slip for both methods.

The method proposed by Osborn *et al.* [7] was implemented as follows: i) the hardware was adjusted to operate at the same sampling rate as used in [7] (260 Hz); ii) the derivative of the force signal for all taxels of the tactile sensor was calculated; iii) whenever any of the taxels detected slip (a fast change in the derivative signal above a threshold - see [7] for further details) the control system of the i-Limb was activated to close the fingers during 45 ms; iv) for each instance of slip, the total time of closure was increased by 45 ms until slip was suppressed. The reaction time was measured as the time elapsed between the onset of the accelerometer signal and the first instance of slippage. The total response time was considered as the total time of closure generated by the algorithm. This method will be referred to, hereafter, as Neuromimetic Slip Detection (NMSD).

The slip detection method proposed by Romeo *et al.* [16] was implemented as follows: i) the sampling rate was adjusted to 380 Hz (same as described in [16]); ii) a stationary wavelet transform (SWT) was applied to the force signals of each taxel to detect fast transient events related to slip - a moving window of 21 ms (8 samples) was used to decompose the force signal into three levels; iii) slip was considered to have occurred if the value of the third level detail coefficient crossed a threshold and movement would continue for at least another 21 ms (see [16] for further details); iv) each taxel was analyzed individually, and the final ON-OFF slip signal was generated by applying a logic OR operation over all the taxels. The reaction time was measured as the time elapsed between the onset of the accelerometer and the start of the ON-OFF signal. Hereinafter, this method will be referred to as SWT-Slip Detection (SWT-SD).

III. Results

The first experiment was designed to investigate the performance of the proposed slip detection technique, using both the fixed threshold and DATH methods. Figs. 6A and 7A present the output of the slip sensor while the test surface was scanned. Figs. 6B-D and 7B-D present detailed views associated with the scanning of the white section of the test surface (defined by the vertical dashed lines in 6A and 7A).

Given the high reflectance of the white surface, the output voltage of the slip sensor oscillated around a low value (300 to 500 mV) (Figs. 6B and 7B). The oscillations were promoted due to relative motion and changes in the reflected light caused by imperfections of the test surface. Nevertheless, these small oscillations were picked up by the slip detection method. The spike generation process consisted of accumulating the difference between consecutive samples, and once the threshold was breached (Figs. 6C and 7C), a spike was fired. As shown, the fixed threshold strategy to detect slip

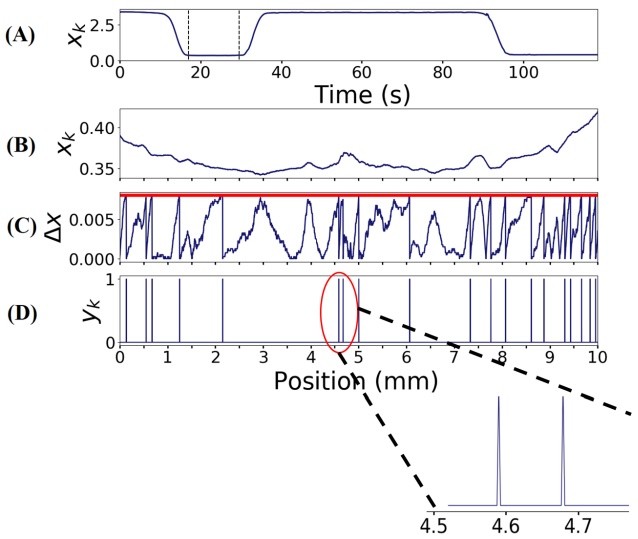

Fig. 6. Characterization experiment while scanning the white portion of the test surface using a fixed threshold for slip detection. A) The filtered output of the slip sensor during the complete experiment. Low amplitudes indicate scanning over the white portion; higher amplitudes indicate the black portion. B) Detailed view of the filtered output of the slip sensor while scanning the white portion. C) Spike generation. The waveform of Δx is shown in blue, and the threshold θ is shown in red. D) Generated spikes according to Eq. 1 and Eq. 2. The region circled in red is shown in detail. The minimum distance observed between two consecutive spikes was equal to 0.09 mm.

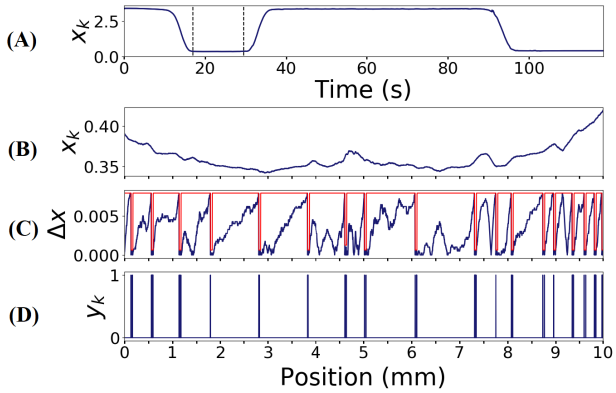

Fig. 7. Characterization experiment while scanning the white portion of the test surface using DATH for slip detection. A) The filtered output of the slip sensor during the complete experiment. Low amplitudes indicate scanning over the white portion; higher amplitudes indicate the black portion. B) Detailed view of the filtered output of the slip sensor while scanning the white portion. C) Spike generation. The waveform of Δx is shown in blue, and the threshold θ is shown in red. DATH changes the value of the threshold briefly after a first spike is detected. D) Generated spikes according to Eq. 1 and Eq. 2.

(Fig. 6D) produced a smaller number of spikes than DATH (Fig. 7D). DATH reduced the threshold θ temporally, which prompted the generation of more spikes after a first one was triggered (Fig. 7C). However, for both cases, the spikes would be generated within a minimum distance of 0.09 mm (Fig. 6D and Fig. 7D).

Figs. 8A and 9A present the output of the slip sensor while the test surface was scanned. Figs. 8B-D and 9B-D present detailed views associated with the scanning of the black section of the test surface (defined by the vertical dashed lines in 8A and 9A). Given its low reflectance, the overall voltage

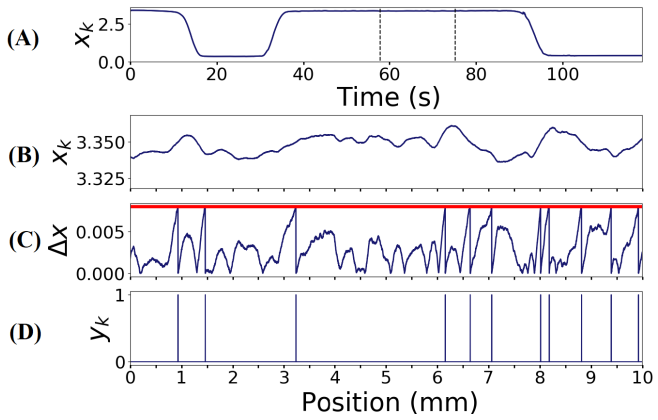

Fig. 8. Characterization experiment while scanning the black portion of the test surface using a fixed threshold for slip detection. A) The filtered output of the slip sensor during the complete experiment. Low amplitudes indicate scanning over the white portion; higher amplitudes indicate the black portion. B) Detailed view of the filtered output of the slip sensor while scanning the black portion. C) Spike generation. The waveform of Δx is shown in blue, and the threshold θ is shown in red. D) Generated spikes according to Eq. 1 and Eq. 2.

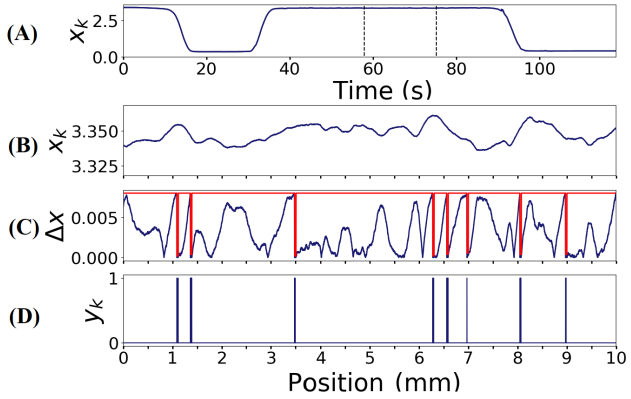

Fig. 9. Characterization experiment while scanning the black portion of the test surface using a fixed threshold for slip detection. A) The filtered output of the slip sensor during the complete experiment. Low amplitudes indicate scanning over the white portion; higher amplitudes indicate the black portion. B) Detailed view of the filtered output of the slip sensor while scanning the black portion. C) Spike generation. The waveform of Δx is shown in blue, and the threshold θ is shown in red. DATH changes the value of the threshold briefly after a first spike is detected. D) Generated spikes according to Eq. 1 and Eq. 2.

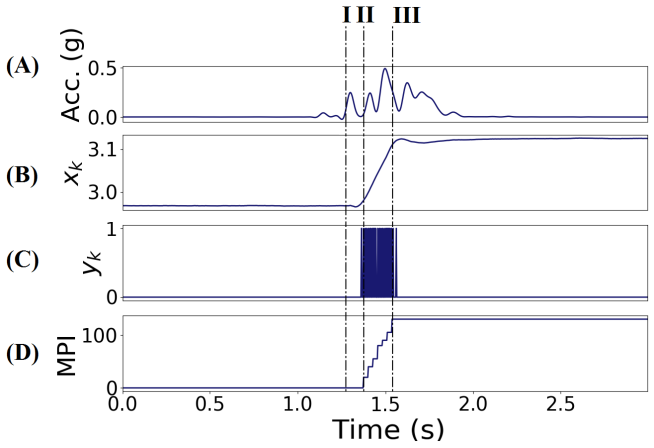

Fig. 10. Results of slip suppression method for the sudden drop of 10 g on the bottle DK using DATH. A) Accelerometer signal (Y-axis). B) The filtered output of the slip sensor. C) Events triggered by the slip of the bottle after dropping the 10 g object inside. D) MPI controller output. The response time was measured as the time elapsed from the onset of the slip signal detected in the accelerometer signal (I) until the first response of the controller (II). The total controller time was measured as the time elapsed from the first response of the controller (II) until its final response when the slip was suppressed (III).

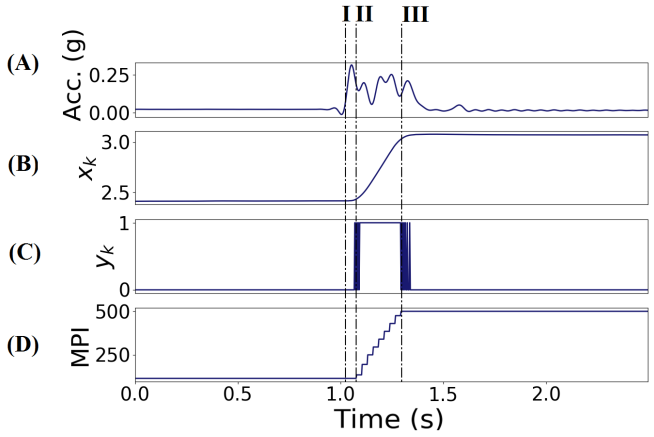

Fig. 11. Results of slip suppression method for the sudden drop of 10 g on the bottle TR using DATH. A) Accelerometer signal (Y-axis). B) The filtered output of the slip sensor. C) Events triggered by the slip of the bottle after dropping the 10 g object inside. D) MPI controller output. The response time was measured as the time elapsed from the onset of the slip signal detected in the accelerometer signal (I) until the first response of the controller (II). The total controller time was measured as the time elapsed from the first response of the controller (II) until its final response when the slip was suppressed (III).

level oscillated around 3.32 and 3.35 V during motion (Fig. 8B and Fig. 9B). Despite the lower reflectance, several spikes were generated and captured by the slip detection method (Figs. 8C-D and Figs. 9C-D). These results demonstrated that it is possible to associate slip-induced motion to changes in the sensor output, triggering events (spikes) that mimic the activity of FA-I afferents.

The experiments with the test surface also showed that the UR10 was capable of maintaining a constant distance between the slip sensor and the surface. The changes in amplitude produced by scanning the white (Figs. 6B and 7B) or black portions (Figs. 8B and 9B) of the test surface were small and did not exhibit any consistent trend that could be indicative of changes in distance or external illumination. Furthermore, spikes were generated based on relative changes in the amplitude of the signal, which is suitable for detecting motion of surfaces with different reflectance properties.

Figs. 10, 11, and 12 illustrate one of the results obtained in the experiment where an object with a mass of 10 g was suddenly dropped inside the bottles TR, DK, and TX. In this experiment, the slip was characterized by a fast-transient event, verified as abrupt changes in the accelerometer signal. As slip occurred, events were generated from the output of the sensor and passed to the MPI controller.

Figs. 13 and 14 present the individual results obtained by employing the fixed threshold strategy, the DATH method, and the NMSD and SWT-SD methods, for the three bottles. DATH improved both slip detection and suppression performance when compared to using a fixed threshold. The

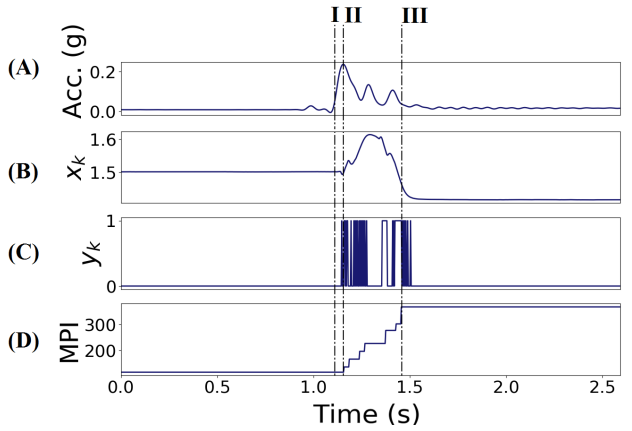

Fig. 12. Results of slip suppression method for the sudden drop of 10 g on the bottle TX using DATH. A) Accelerometer signal (Y-axis). B) The filtered output of the slip sensor. C) Events triggered by the slip of the bottle after dropping the 10 g object inside. D) MPI controller output. The response time was measured as the time elapsed from the onset of the slip signal detected in the accelerometer signal (I) until the first response of the controller (II). The total controller time was measured as the time elapsed from the first response of the controller (II) until its final response when the slip was suppressed (III).

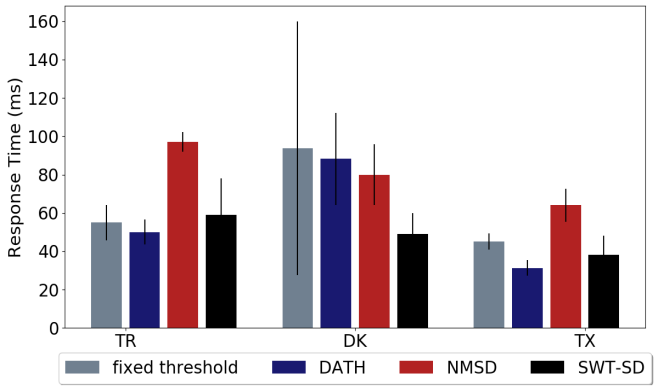

Fig. 13. Response time measured for slip induced by a sudden drop of a 10g object inside the bottles. Vertical bars denote the standard deviation.

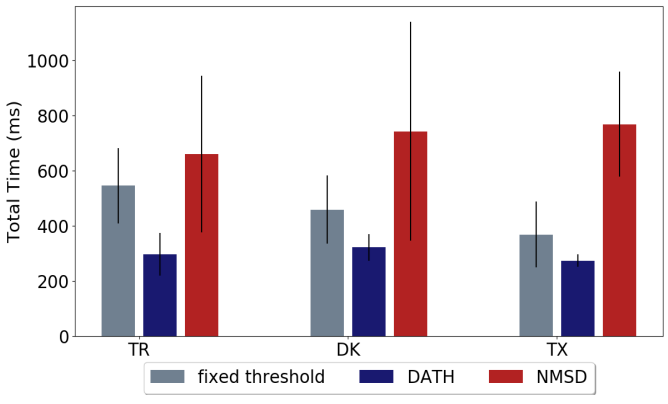

Fig. 14. Total time required for preventing slip induced by a sudden drop of a 10g object inside the bottles. Vertical bars denote the standard deviation.

response time decreased for bottles TR, DK, and TX (DATH: 50 ± 6.48 ms, 88.2 ± 24 ms and 31.3 ± 4.16 ms, respectively; fixed threshold: 55 ± 9.16 ms, 93.75 ± 66 ms and 45 ± 4.24 ms, respectively). The fixed threshold strategy showed a poor performance in preventing slip (less than 50% of successful trials). However, by employing DATH, the number

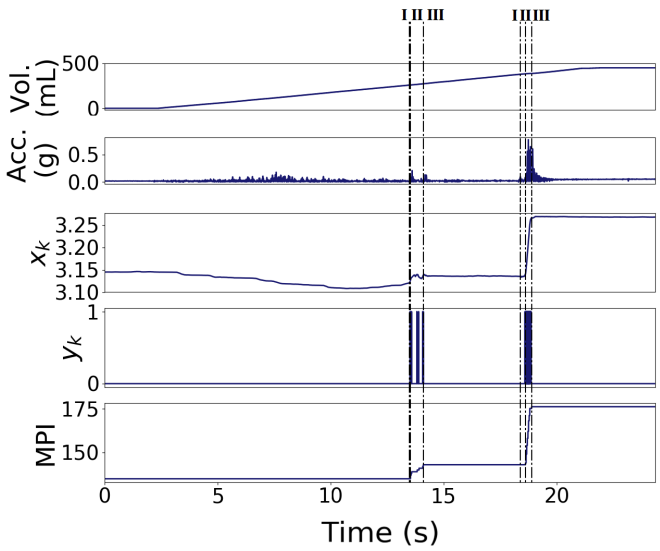

Fig. 15. Results obtained for the DATH slip suppression method when pouring 500 ml of water in bottle DK. A) Water volume estimated from the output of the water flow sensor. B) Accelerometer signal. C) The filtered output of the slip sensor. D) Events triggered by the slippage of the bottle. E) MPI controller output. The response time was measured as the time elapsed from the onset of the slip signal detected in the accelerometer signal (I) until the first response of the controller (II). The total controller time was measured as the time elapsed from the first response of the controller (II) until its final response when the slip was entirely suppressed (III). Gradual increase of the weight of the bottle induced two distinct slips with the second being more pronounced due to a higher load.

of successful trials increased to 80% on average, which is also associated with the decrease in the total time required for completely suppressing slip. Note that, for the textured bottle (TX), DATH showed the best results, where complete slippage was prevented in 90% of the trials and took the least amount of time to suppress slip (DATH: 274.4 ± 22.51 ms).

In comparison with SWT-SD and NMSD, DATH performed better for the majority of the cases, showing faster reaction time for bottles TR and TX. For the dark bottle (DK), SWT-SD showed the fastest response. Nevertheless, the average reaction time of DATH, as well as NMSD and SWT-SD, for all bottles, are still similar to human reaction time, at around 80 ms [4], [5].

In terms of the total time required to suppress object slippage, DATH performed consistently better than the NMSD and fixed threshold strategies. The total time required to suppress slip by NMSD was, on average, more than twice of that achieved by DATH [(TR: DATH = 298.5 ± 77.41 ms, NMSD = 661 ± 283 ms), (DK: DATH = 322.5 ± 48.15 ms, NMSD = 743 ± 396.5 ms) and (TX: DATH = 273 ± 22.51 ms, NMSD = 769 ± 191 ms)].

The second experiment consisted of gradually pouring 500 mL of water into each bottle, dynamically changing their weight over time. Fig. 15 presents one trial for the DK bottle and Figs. 16 and 17 present the overall results for response time and total time to suppress slip, respectively.

Fig. 15 shows that, as the water was poured, the first slip occurred at about 200 ml, and the second event occurred when the bottle was filled with about 400 ml of water. This subsequent event provides evidence that the MPI controller was capable of suppressing slip by applying just

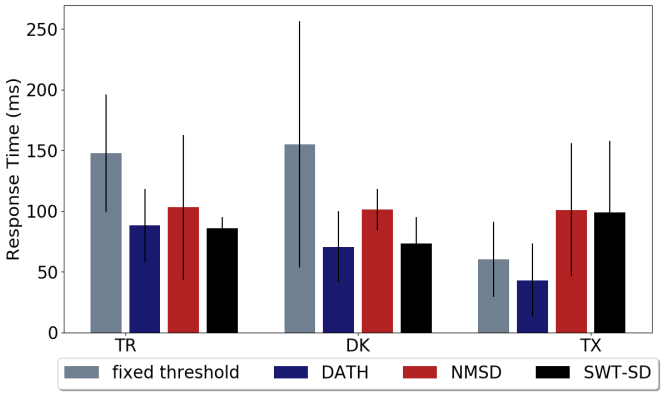

Fig. 16. Response time to slip induced by pouring 500 mL in the bottles. Vertical bars denote the standard deviation.

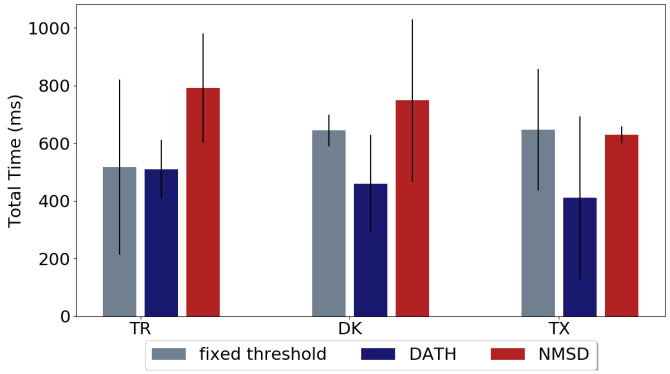

Fig. 17. Total time required to fully suppress the slip induced by pouring 500 mL of water in the bottles. Vertical bars denote the standard deviation.

enough force for each specific event, avoiding excessive and unnecessary grip force. Thus, as the weight increased, further slips occurred and had to be corrected by the controller.

In these experiments, slippage was characterized as a slower component due to the gradual increase in object weight. There was an increase in the reaction time for all methods (Fig. 16) when compared to the previous experiments. However, the overall trends persist. For bottle TR, DATH and SWT-SD showed a faster response when compared to the NMSD and fixed threshold strategies (DATH: 88 $\pm$ 30 ms, SWT-SD: 86 $\pm$ 9 ms, NMSD: 103 $\pm$ 59 ms, fixed threshold: 147.75 $\pm$ 48.45 ms). For bottle DK, DATH and SWT-SD showed a similar response time, and both were again faster than NMSD and the fixed threshold (DATH: 70 $\pm$ 29.4 ms, SWT-SD: 73 $\pm$ 22 ms, NMSD: 100 $\pm$ 17 ms, fixed threshold: 155 $\pm$ 101.52 ms). DATH showed the fastest response time for bottle TX (43 $\pm$ 30.34 ms, fixed threshold: 60 $\pm$ 30.9 ms).

In terms of the total time required to suppress object slippage while the water was poured in the bottles (Fig. 17), DATH again performed consistently better than NMSD and the fixed threshold [(TR: DATH = 509 $\pm$ 102 ms, NMSD = 792 $\pm$ 192 ms, Fixed threshold = 509 $\pm$ 102.45 ms), (DK: DATH = 460 $\pm$ 168 ms, NMSD = 749 $\pm$ 281 ms, Fixed threshold = 460 $\pm$ 168.47 ms) and (TX: DATH = 411 $\pm$ 282 ms, NMSD = 630 $\pm$ 29 ms, Fixed threshold =: 411.66 $\pm$ 282.68 ms)]. Furthermore, DATH successfully prevented complete slippage in all trials.

IV. Discussion

In this paper, a bio-inspired approach for detecting and suppressing slippage was presented. The output of an optical sensor was converted into events that represent the activity of FA-I afferents. The response of the slip sensor was characterized using a test surface that contained minimum (white) and maximum reflectance (black) portions. Linear motion, without changes in distance between the slip sensor and the test surface, promoted oscillations in the output of the sensor. The oscillations were attributed to surface features and were successfully captured by the proposed bio-inspired slip detection method. The results showed that spikes could be generated after relative movements (slip) as low as 0.09 mm. The results have also provided experimental validation of the MPI control law performance for successfully suppressing slippage of three different bottles, in two proof of concept experiments. In a previous work, it was found that the event-based slip detection method was sensitive to the reflectance properties of objects [27]. Here, the framework was extended with the addition of the DATH method, demonstrating that it is possible to overcome the limitations imposed by more challenging surfaces. DATH properly detected and suppressed motion caused by slippage of three different surfaces (TR, DK, and TX) that are representative of several objects. In that sense, DATH can be used as a more general slip detection method, capable of producing robust overall behavior, regardless of the surface.

The bio-inspired approach followed the principles of neuromorphic sensing. This strategy proved to be beneficial, as it was capable of filtering noise and avoiding possible false positives, while also rendering the method insensitive to the actual voltage level of the sensor, which is modulated according to the properties of the different surfaces. Spikes or events were generated only in the presence of object motion caused by a slip, generating discrete spikes akin to the behavior of biological FA-I receptors [5]. The human tactile sensory system is indeed far more complex and uses signals from other afferents such as SA-I and FA-II cells, that are also involved in biological slip detection and prevention. Although very exciting and promising, it is beyond the scope of this paper to fully mimic the complex spiking activity of all mechanoreceptors and their respective functions. Furthermore, since SA-I afferents also encode static forces, these cells generally produce spikes while objects are being held, even in the absence of motion [20]. Such feature is not compatible with the proposed MPI controller, which is tuned to respond to spikes that are related to motion alone. Consequently, a biomimetic approach that makes use of SA-I would require to discriminate between spikes that are related to gripping from those that are related to slip – although this is not an impossible task, it would add unnecessary steps and complexity to the method. Besides, spikes that are not related to motion would trigger the controller to generate undesired grip force adjustments from the prosthetic hand. Finally, the setpoint for the proposed controller is equal to zero. Since slips generate the spikes, the controller acts to suppress motion by reducing the number of spikes to zero. As such, the behavior of FA-I afferents is the most related

approach to provide the transient tactile input required for the MPI controller.

The proposed slip detection method is based on capturing changes in the amount of light reflected by the objects due to surface anisotropies. Other works have focused on capturing the deformation of a soft layer during contact with objects [28]–[30]. That is an interesting approach to optical-based tactile sensing, since it is not affected by changes in the reflectance properties of the surfaces or ambient light, and it is capable of reproducing texture details in high resolution. However, these systems are still bulky and might demand customized end-effectors given the size of the cameras or the slip sensor itself [12]. Thus, incorporating such sensors into the fingers of prosthetic hands is not straightforward [11]. In this paper, it was demonstrated the benefit of using an optical approach for detecting slip using a miniaturized sensor that can be assembled into prosthetic hands. Investigating slip detection with slip sensors that are embedded in a soft skin with less sensing elements is a possible future direction for this work, preserving its bio-inspired aspects, while also evolving sensor design [31].

The slip suppression experiments provided evidence that that the modified version of the MPI control law was robust enough to properly maintain hold of objects under two different dynamic slip conditions. The first experiment tested the response to a sudden perturbation, generating unidirectional slip. The second experiment tested the response to a gradual, constant perturbation, which promoted both uniaxial and rotational slips. Despite such differences, the MPI control law was capable of successfully preventing complete slippage of the bottles in most of the trials for both experiments.

It should be noted that the proposed method responds to motion. Thus, a certain amount of slip should be expected. Nonetheless, throughout the experiments, the DATH method was capable of achieving an overall response time of less than 85 ms. This response time is similar to the human reaction time to slip [4] and, once again, demonstrates the effectiveness of the method. Besides, the proposed controller takes a continuous signal as input, generating gradual grip force adjustments as long as the object is slipping. In this sense, the method can be applied in future prosthetic devices, serving as a low-level reflex mechanism to prevent the slippage of objects without explicit action from the user.

The performance of the proposed method was compared with a biomimetic method for slip detection and suppression [7] and with a non-biomimetic slip detection method [16]. The results showed that DATH performed consistently better for the majority of the cases, successfully preventing complete slippage in all trials.

Overall, the results demonstrate that this novel approach to neuromorphic touch can be used to support grasping for robotic manipulators. The method can also be complementary to force sensors in order to capture and suppress slip since it is based on detecting sliding motion of objects, which is harder to achieve with standard force sensors due to the breaking of contact between the object and the manipulator. In fact, a multi-modal approach could be beneficial for building more robust tactile systems where the activity of Pacinian receptors tuned to vibrations could also be encoded [32]. Furthermore, the event-based control system could be improved and expanded into a fully neuromorphic system, following models of motoneurons and muscle fibers [33], building a complete bio-inspired robotic solution.

V. Conclusion

In this paper, a bio-inspired approach for detecting and suppressing slip was presented. The method takes advantage of the capacity of miniature optical sensors to accurately track the motion of objects within its field of view. The proposed event-based control system was capable of promoting a reflex-like response that is proportional to slip. This approach can be potentially useful in many applications where standard motion sensors, such as accelerometers, show unreliable responses due to various environmental issues, such as vibration, and in the case of low friction surfaces where no vibration would be detected as the object slides out of the grip.

Acknowledgment

The statements made herein are solely responsibility of the authors. The funders had no role in the study design, data collection and analysis or preparation of the manuscript.

References

[1] K. O. Johnson and S. S. Hsiao, "Neural mechanisms of tactual form and texture perception," *Annu. Rev. Neurosci.*, vol. 15, no. 1, pp. 227–250, Mar. 1992.

[2] D. Prattichizzo and J. C. Trinkle, "Springer handbook of robotics," in *Grasping*. Berlin, Germany: Springer, 2008, pp. 671–700. [Online]. Available: https://link.springer.com/referenceworkentry/10.1007%2F978-3-540-30301-5_29

[3] G. Westling and R. S. Johansson, "Factors influencing the force control during precision grip," *Exp. Brain Res.*, vol. 53, no. 2, pp. 277–284, Jan. 1984.

[4] G. Westling and R. S. Johansson, "Responses in glabrous skin mechanoreceptors during precision grip in humans," *Exp. Brain Res.*, vol. 66, no. 1, pp. 128–140, Mar. 1987.

[5] R. S. Johansson and G. Westling, "Signals in tactile afferents from the fingers eliciting adaptive motor responses during precision grip," *Exp. Brain Res.*, vol. 66, no. 1, pp. 141–154, Mar. 1987.

[6] R. S. Dahiya, G. Metta, M. Valle, and G. Sandini, "Tactile sensing—From humans to humanoids," *IEEE Trans. Robot.*, vol. 26, no. 1, pp. 1–20, Feb. 2010.

[7] L. Osborn, R. R. Kaliki, A. B. Soares, and N. V. Thakor, "Neuromimetic event-based detection for closed-loop tactile feedback control of upper limb prostheses," *IEEE Trans. Haptics*, vol. 9, no. 2, pp. 196–206, Apr./Jun. 2016.

[8] M. Rasouli, Y. Chen, A. Basu, S. L. Kukreja, and N. V. Thakor, "An extreme learning machine-based neuromorphic tactile sensing system for texture recognition," *IEEE Trans. Biomed. Circuits Syst.*, vol. 12, no. 2, pp. 313–325, Apr. 2018.

[9] L. E. Osborn *et al.*, "Prosthesis with neuromorphic multilayered e-dermis perceives touch and pain," *Sci. Robot.*, vol. 3, no. 9, Jun. 2018, Art. no. eaat3818.

[10] H. Dang and P. K. Allen, "Learning grasp stability," in *Proc. IEEE Int. Conf. Robot. Autom.*, May 2012, pp. 2392–2397.

[11] M. T. Francomano, D. Accoto, and E. Guglielmelli, "Artificial sense of slip—A review," *IEEE Sensors J.*, vol. 13, no. 7, pp. 2489–2498, Jul. 2013.

[12] W. Chen, H. Khamis, I. Birznieks, N. F. Lepora, and S. J. Redmond, "Tactile sensors for friction estimation and incipient slip detection—Toward dexterous robotic manipulation: A review," *IEEE Sensors J.*, vol. 18, no. 22, pp. 9049–9064, Nov. 2018.

[13] J. Tegin and J. Wikander, "Tactile sensing in intelligent robotic manipulation—A review," *Ind. Robot*, vol. 32, no. 1, pp. 64–70, Feb. 2005.

[14] Y. Zhang, X.-G. Duan, G. Zhong, and H. Deng, "Initial slip detection and its application in biomimetic robotic hands," *IEEE Sensors J.*, vol. 16, no. 19, pp. 7073–7080, Oct. 2016.
[15] R. A. Romeo, C. M. Oddo, M. C. Carrozza, E. Guglielmelli, and L. Zollo, "Slippage detection with piezoresistive tactile sensors," *Sensors*, vol. 17, no. 8, p. 1844, Aug. 2017.
[16] R. A. Romeo *et al.*, "Identification of slippage on naturalistic surfaces via wavelet transform of tactile signals," *IEEE Sensors J.*, vol. 19, no. 4, pp. 1260–1268, Feb. 2019.
[17] H. N. Sani and S. G. Meek, "Characterizing the performance of an optical slip sensor for grip control in a prosthesis," in *Proc. IEEE Int. Conf. Intell. Robot. Syst.*, Sep. 2011, pp. 1927–1932.
[18] L. Roberts, G. Singhal, and R. Kaliki, "Slip detection and grip adjustment using optical tracking in prosthetic hands," in *Proc. Annu. Int. Conf. IEEE Eng. Med. Biol. Soc. (EMBS)*, Aug./Sep. 2011, pp. 2929–2932.
[19] R. S. Johansson and G. Westling, "Programmed and triggered actions to rapid load changes during precision grip," *Exp. Brain Res.*, vol. 71, no. 1, pp. 72–86, Jun. 1988.
[20] J. M. Romano, K. Hsiao, G. Niemeyer, S. Chitta, and K. J. Kuchenbecker, "Human-inspired robotic grasp control with tactile sensing," *IEEE Trans. Robot.*, vol. 27, no. 6, pp. 1067–1079, Dec. 2011.
[21] R. S. Johansson and J. R. Flanagan, "Coding and use of tactile signals from the fingertips in object manipulation tasks," *Nature Rev. Neurosci.*, vol. 10, no. 5, pp. 345–359, Apr. 2009.
[22] Z. Su *et al.*, "Force estimation and slip detection/classification for grip control using a biomimetic tactile sensor," in *Proc. IEEE-RAS Int. Conf. Humanoid Robot.*, Nov. 2015, pp. 297–303.
[23] A. Prach, J.-J. Cabibihan, N. V. Thakor, and D. S. Bernstein, "Pareto-front analysis of a monotonie PI control law for slip suppression in a robotic manipulator," in *Proc. IEEE Int. Conf. Robot. Biomimetics (ROBIO)*, Dec. 2018, pp. 2728–2733.
[24] L. S. Smith, "Neuromorphic systems: Past, present and future," in *Brain Inspired Cognitive Systems* (Advances in Experimental Medicine and Biology). New York, NY, USA: Springer, 2010.
[25] U. B. Rongala, A. Mazzoni, and C. M. Oddo, "Neuromorphic artificial touch for categorization of naturalistic textures," *IEEE Trans. Neural Netw. Learn. Syst.*, vol. 28, no. 4, pp. 819–829, Apr. 2017.
[26] W. W. Lee, H. Yu, and N. V. Thakor, "Gait event detection through neuromorphic spike sequence learning," in *Proc. 5th IEEE RAS/EMBS Int. Conf. Biomed. Robot. Biomechatronics*, Aug. 2014, pp. 899–904.
[27] A. Nakagawa-Silva, S. P. Reddy Sunkesula, A. Prach, J.-J. Cabibihan, N. V. Thakor, and A. B. Soares, "Slip suppression in prosthetic hands using a reflective optical sensor and MPI controller," in *Proc. IEEE Biomed. Circuits Syst. Conf. (BioCAS)*, Oct. 2018, pp. 1–4.
[28] W. Yuan, R. Li, M. A. Srinivasan, and E. H. Adelson, "Measurement of shear and slip with a GelSight tactile sensor," in *Proc. IEEE Int. Conf. Robot. Automat.*, May 2015, pp. 304–311.
[29] S. Dong, W. Yuan, and E. H. Adelson, "Improved GelSight tactile sensor for measuring geometry and slip," in *Proc. IEEE Int. Conf. Intell. Robots Syst.*, Sep. 2017, pp. 137–144.
[30] J. W. James, N. Pestell, and N. F. Lepora, "Slip detection with a biomimetic tactile sensor," *IEEE Robot. Autom. Lett.*, vol. 3, no. 4, pp. 3340–3346, Oct. 2018.
[31] A. Cirillo, P. Cirillo, G. De Maria, C. Natale, and S. Pirozzi, "An artificial skin based on optoelectronic technology," *Sens. Actuators A, Phys.*, vol. 212, pp. 110–122, Jun. 2014.
[32] P. Mittendorfer and G. Cheng, "Humanoid multimodal tactile-sensing modules," *IEEE Trans. Robot.*, vol. 27, no. 3, pp. 401–410, Jun. 2011.
[33] C. M. Niu, K. Jalaleddini, W. J. Sohn, J. Rocamora, T. D. Sanger, and F. J. Valero-Cuevas, "Neuromorphic meets neuromechanics, part I: The methodology and implementation," *J. Neural Eng.*, vol. 14, no. 2, Feb. 2017, Art. no. 025001.

Andrei Nakagawa-Silva received the B.S. degree in mechanical and biomedical engineering and the M.Sc. degree in biomedical engineering from the Federal University of Uberlandia, Uberlandia, Brazil, in 2012 and 2015, respectively, where he is currently pursuing the Ph.D. degree. His main research focuses on somatosensory system integration and the development and implementing tactile sensing technologies and algorithms for use with robotic and prosthetic limbs.

Nitish V. Thakor (F'94–LF'18) is a Professor of Biomedical Engineering, Electrical and Computer Engineering, and Neurology at Johns Hopkins University and directs the Laboratory for Neuroengineering. He is also a Professor at the Singapore Institute for Neurotechnology (SINAPSE), National University of Singapore. His technical expertise is in the field of neuroengineering, including neural diagnostic instrumentation, neural microsystems, neural signal processing, optical imaging of the nervous system, neural control of prosthesis, and brain–machine interface. He has authored more than 300 refereed journal publications. He is a Fellow of the American Institute of Medical and Biological Engineering, the Founding Fellow of the Biomedical Engineering Society, and the Fellow of the International Federation of Medical and Biological Engineering. He was a recipient of the Research Career Development Award from the National Institutes of Health and the Presidential Young Investigator Award from the U.S. National Science Foundation. He was the Editor-in-Chief of the IEEE TRANSACTIONS ON NEURAL SYSTEMS AND REHABILITATION ENGINEERING. He is presently the Editor-in-Chief of *Medical and Biological Engineering and Computing*.

John-John Cabibihan (SM'14) received the Ph.D. degree in bioengineering, with specialization in biorobotics, from Scuola Superiore Sant'Anna, Pisa, Italy, in 2007. From 2008 to 2013, he was an Assistant Professor with the Electrical and Computer Engineering Department, National University of Singapore. He is currently an Associate Professor with the Department of Mechanical and Industrial Engineering, Qatar University. He is also the Lead/Co-Lead Principal Investigator of several projects under the National Priorities Research Program of Qatar National Research Fund. He is an Associate Editor/Editorial Board Member of the IEEE ROBOTICS AND AUTOMATION LETTERS, *Frontiers in Bioengineering and Biotechnology*, *International Journal of Advanced Robotics Systems*, and *Springer Nature Applied Sciences Journal*.

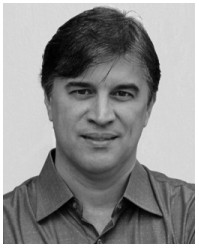

Alcimar B. Soares (M'13) received the B.S. degree in electrical engineering and the M.Sc. degree in artificial intelligence from the Federal University of Uberlandia, Brazil, in 1987 and 1990, respectively, and the Ph.D. degree in biomedical engineering from The University of Edinburgh, U.K., in 1997. He is currently a Full Professor and the Head of the Biomedical Engineering Laboratory, Faculty of Electrical Engineering, Federal University of Uberlandia. His research interests include the modeling and estimation of neuromotor control systems, large-scale neural systems dynamics, targeted neuroplasticity, decoding neural activity, brain–machine interfaces and rehabilitation, and assistive devices. He is also a member of various scientific societies, such as the IEEE Engineering in Medicine and Biology Society, the International Society of Electromyography and Kinesiology, the Brazilian Society of Biomedical Engineering, and the Brazilian Society of Electromyography and Kinesiology. He is the Editor-in-Chief of the *Research on Biomedical Engineering* journal, the Deputy Editor of the *Medical & Biological Engineering & Computing* journal, and an Associate Editor of the *Journal of Biomedical Engineering and Biosciences*.